12th International Conference on Fracture Mechanics of Concrete and Concrete Structures
FraMCoS-12
B.L.A. Pichler, Ch. Hellmich, P. Preinstorfer (Eds)

https://doi.org/10.21012/FC12.1157
MS06-3:1

MICROMECHANICAL CHARACTERIZATION OF THE INTERFACIAL TRANSITION ZONE IN RECYCLED BRICK CONCRETE BY MEANS OF COMBINED NANOINDENTATION AND SEM

FENG LI[1], FLORIAN KLEINER[2], CHRISTIANE RÖSSLER[2], LUISE GÖBEL[2,3] AND ELSKE LINSS[1]

[1] Material Research and Testing Institute Weimar
Coudraystraße 9, Weimar, 99423, Germany
e-mail: feng.li@mfpa.de

[2] F. A. Finger Institute for Building Material Science, Bauhaus-Universität Weimar
Coudraystraße 11A, Weimar, 99423, Germany

[3] Institute of Structural Mechanics, Bauhaus-Universitäty Weimar,
Marienstraße 13, Weimar, Germany

Key words: Recycled concrete, Brick aggregate, Interfacial transition zone, Nanoindentation

Abstract: The interfacial transition zone (ITZ), which is the weakest component of concrete, is inherently complex due to its spatially varying heterogeneity. It is therefore essential to gain a deeper understanding of the relationship between the microstructural characteristics and the macroscopic mechanical properties. In this context, the quality and resolution of both microscopic and micromechanical testing techniques have been improved, and nanoindentation has become an accepted measurement method for determining the micromechanical properties of materials. In the present study, nanoindentation is combined with scanning electron microscopy (SEM) to investigate the ITZ of recycled concrete made from recycled brick aggregate. The measurement procedure was adapted as follows: three suitable areas of ITZ and one additional area of bulk paste were selected for further analysis using optical light microscope. These areas were subsequently analyzed using SEM to identify and characterize the ITZ. Based on the image analysis, the distribution of porosity was determined. Nanoindentation grids with 5 µm spacing were then applied to the areas. In addition, deconvolution analysis of the probability density function obtained from more than 700 indentation results in each ITZ and bulk paste allows the quantitative characterization of the identified phases. The porosity analysis shows that the ITZ thickness is 65 µm, and the porosity of the ITZ is twice that of the bulk paste. The nanoindentation result shows that the porosity, low density calcium silicate hydrate, and calcium hydroxide are higher in the ITZ, while high density calcium silicate hydrate is higher in the bulk paste. The results provide a fundamental basis for the wider use of recycled brick aggregates in construction.

1 INTRODUCTION

As a heterogeneous material, concrete consists of different phases, such as aggregate, cement paste, and interfacial transition zone (ITZ). Among these, the ITZ is the critical factor affecting the mechanical properties and durability of concrete [1]. The microstructures of the ITZ are similar to those of the cement bulk paste. They consist of different phases such as pores, calcium silicate hydrate (C-S-H), calcium hydroxide (CH), and residual cement clinker.

Due to the high magnification and resolution of the scanning electron microscopy

(SEM), the microstructure can be observed. The study by *Diamond* [2] provided a clear assessment of the microstructure of concrete. Another advantage of this technique is the quantitative analysis of different phases. *Elsharief et al.* [3] studied the distribution of porosity and residual cement clinker from the aggregate surface using cut strips. *Gao et al.* [4] used a method of concentric expansion to study the distribution of porosity. Based on the distribution of porosity, the thickness of ITZ can be determined. These methods are based on SEM image analysis. The principle behind this process is the separation of phases based on the different grey levels present within the binary map. Taking into account the dimensions of the phases, the images need to have a high resolution. In addition to SEM, nanoindentation is also used to investigate the micromechanical properties of concrete. Based on the theory of *Oliver and Pharr* [5], the indentation modulus and hardness can be calculated from the stiffness and indentation depth. Statistical analysis of the results using indentation grids allows the determination of the different phases and the corresponding volume fractions. According to the indentation modulus and hardness from low to high, the range is pore, low density C-S-H (LD C-S-H), high density C-S-H (HD-C-S-H), calcium hydroxide (CH), and residual cement clinker [6-8]. By comparing the difference in micromechanical properties in ITZ and bulk paste, it is possible to determine the thickness of the ITZ. Xiao et al. [9] reported that the thickness of the ITZ between old and new cement paste in recycled concrete is about 55-65 μm, and the nanoindentation modulus of the new ITZ is about 80-90 % of that of the bulk paste. It should be recognized that the micromechanical properties with a large dispersion could affect the result. In addition, the large space between two indentations can lead to a lack of precision.

This paper presents the combined application of SEM and the nanoindentation technique to investigate the ITZ in recycled concrete made with brick aggregate. A comparative assessment of the material properties of the phases found within the ITZ and the bulk phase is then carried out.

2 MATERIALS AND METHODS

2.1 Cement and aggregate

Portland cement type CEM I 42.5R (Thomas Zement GmbH & Co. Kg, Germany) was used for the concrete. The chemical composition of the cement is given in **Table 1**. The used recycled brick aggregates with a size of 4-16 mm, were obtained from a recycling plant and produced by crushing and screening of demolition waste. The bulk density is 1957 kg/m^3 and the water absorption after 10 minutes is 9.3 wt.%.

Table 1: Chemical composition of the cement.

Composition	Fraction (wt.%)
SiO_2	18.99
Fe_2O_3	3.08
Al_2O_3	5.33
CaO	61.45
MgO	1.87
SO_3	3.56
Loss on ignition	3.73

2.2 Sample preparation

The concrete mix has been designed using the absolute volume method. It consists of 70 % by volume fine natural aggregate (0-4 mm) and 30 % by volume brick aggregate (4-16 mm). The concrete mix proportions are shown in **Table 2**. It should be noted that additional water was added to the RC to compensate for the water absorbed by the recycled brick aggregates after 10 minutes. Thus, the effective water/cement ratio of the concrete was therefore 0.55. All aggregates were dried at 105 °C for 24 hours before production. The concrete was then cured in water at room temperature. After 91 days, a disc (diameter ≤ 25 mm, height ≤ 10 mm) was cut from the concrete cubes. To prevent further hydration, the disc was impregnated with isopropanol. It was then dried in a vacuum at room temperature for 24 hours until it reached a

constant mass. The dried specimen was embedded in epoxy resin. Finally, the samples were grinded and polished with diamond paste (down to 0.25 µm).

Table 2: Mixing proportions of concrete.

Material	Proportion (kg/m^3)
Fine natural aggregate (0/4 mm)	1232.7
Recycled brick aggregate (4/16 mm)	394.5
Cement	350.0
Water	192.5
Additional water[a]	36.9

[a.] The additional water is the absorbed water by aggregates after 10 min.

2.3 Testing methods

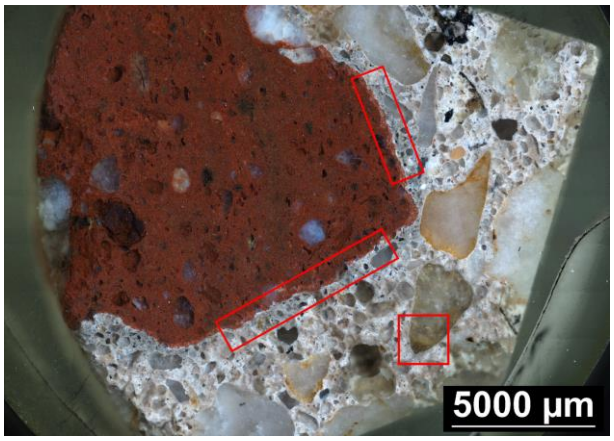

Figure 1: The pre-marked areas in the concrete.

High resolution images of the concrete surface were taken using an microscope (LV100ND, Nikon). Three areas were pre-marked in the acquired image (**Fig. 1**). Two areas contain the interface between the brick aggregate and the paste. One area contains the cement paste. Backscattered electron (BSE) images of the pre-marked areas were acquired using a scanning electron microscope (Helios G4UX, Thermo Fischer Scientific). The interfacial transition zones of aggregates between adjacent aggregates show an overlapping effect, resulting in regionally high pore clustering. It is therefore necessary to select representative regions in the BSE image for the further nanoindentation investigation. The thickness of the ITZ is typically determined to be around 100 µm. Consequently, the dimensions of the selected representative region are 100 × 200 µm^2. It should be noted that no significant aggregates are present in this region.

The nanoindenter (Hysitron TS 77 Select, Bruker) was used to determine the nanoindentation modulus (M) and hardness (H). The Berkovich tip was calibrated on a standard quartz glass surface. To analyze such small phases, the penetration depth (h) must be limited. However, due to the stability of the nanoindentation, the depth should not be too small, with a minimum depth of at least 1/3 of the radius of the indentation tip. The Berkovich tip used has a radius of about 150 nm, and the maximum indentation depth must be at least 50 nm. In addition, the root mean square (*RMS*) of the roughness of the sample surface will affect the results of the test. However, there is no uniformity in the requirements for indentation depth. The experimental results of *Donnelly et al.* [10] showed that h/RMS greater than 3 is reliable. For these reasons, the used maximum loading force used for the study is 2 mN, at which the maximum penetration depth in cement paste is in the range of 200-350 nm [11-13]. The *RMS* roughness of the samples was measured using the Scanning Probe Microscopy in the nanoindenter. Ten different areas on the cement paste were randomly selected for scanning. Each scanning area was set to 50 × 50 µm^2. The measured RMS roughness was 107.9 ± 18.9 nm, remaining below one-third of the maximum penetration depth, thereby meeting the testing criteria. For the ITZ between brick aggregate and paste, three representative regions were investigated using a grid nanoindentation. The grid was divided into 20 rows and 40 columns with a spacing of 5 µm per indent. Consequently, 800 indentations were made for each region tested. An additional region was tested between natural aggregate and cement paste. A 30 × 30 grid nanoindentation was performed in this region. Each indentation was performed under load control. It was first loaded to a maximum load of 2 mN in 5 s, held at the maximum load

for 2 s to minimize the effect of creep, and finally unloaded in 5 s. The raw data was processed for subsequent analysis of micromechanical properties.

After nanoindentation, SEM-BSE images were taken again to identify the identations and the corresponding hardness and indentation modulus of each phase.

3 RESULTS AND DISSCUSION

3.1 Microstructure

Fig. 2 shows the SEM-BSE images from one of the interfaces between brick aggregate and cement paste. The brick aggregate is clearly visible in the image based on its shape. Between the two white lines is the ITZ, which has a significantly high porosity. Notably, there are also microcracks around the aggregate. The area left by the aggregate and ITZ appears compact. This can be defined as bulk paste.

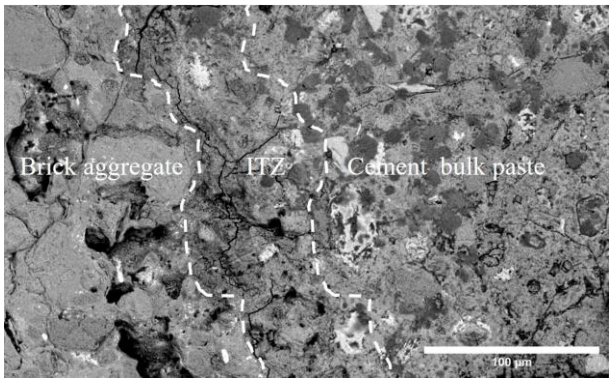

Figure 2: The SEM-BSE images from one of the representative interfaces between brick aggregate and cement paste at magnification of 500×. Dimension: 350 × 211 µm^2.

To evaluate the porosity around the brick aggregate, seven representative regions (dimension: about 150 × 211 µm^2) were selected from a BSE image with a dimension of 4.3 × 1.3 mm^2 at 400× magnification. The porosity determination was based on a grey level segmentation using the software 'ImageJ'. The interface line was drawn manually after segmentation of the aggregates. The cumulative histogram method was used to determine the upper threshold grey values for pore segmentation in the vicinity of the aggregates. The lower inflection point, which is the intersection of two tangents, can be considered as the upper threshold for pores [4]. The porosity distribution was determined by strip delineation (with a 1 µm spacing), starting from the interface line. The result is shown in **Fig. 3**.

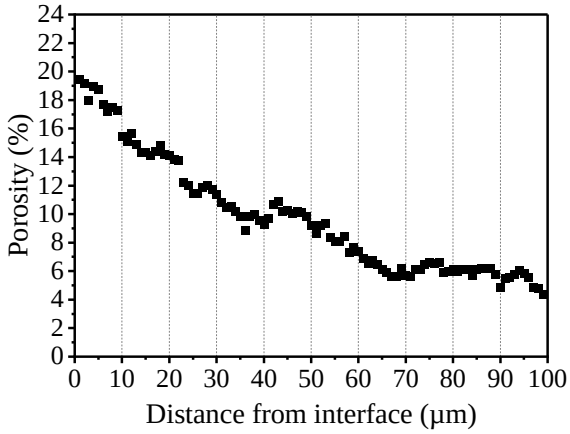

Figure 3: Distribution of average porosity 100 µm away from the interface of brick aggregate.

The highest porosity, approximately 20 %, is observed within a few microns from the interface. The porosity tends to gradually decrease until it finally levels off with increasing distance. The inflection point is defined as the boundary between the ITZ and the bulk paste. Therefore, the ITZ thickness can be calculated to be 65 µm. The porosity in the bulk paste is about 5.8 %. The average porosity in the ITZ is approximately 11.7 %, which is twice that of the bulk paste.

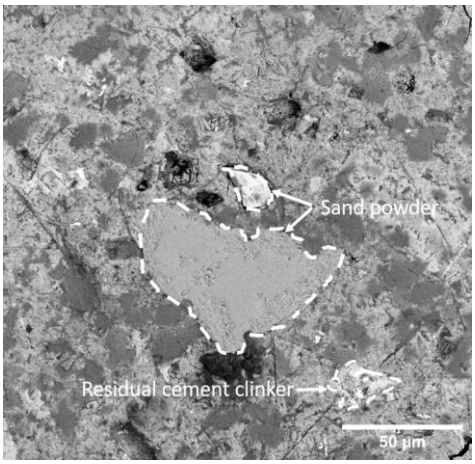

Figure 4: The SEM-BSE images from cement paste at a magnification of 1000×. Dimension: 194 × 183 µm^2.

The bulk paste image was taken in the area, which is at least 100 µm away from the nearest aggregate. As shown in **Fig. 4**, the sand powder and residual cement clinker can be observed. The separation of cement hydrate products remains a challenging endeavor due to their overlapping morphologies.

3.2 Micromechanical properties

The contour plots in **Fig. 5** show the measured indentation modulus (M) and hardness (H) of the investigated area in **Fig. 2**. The contour plots exhibit a clear correlation with the microstructure.

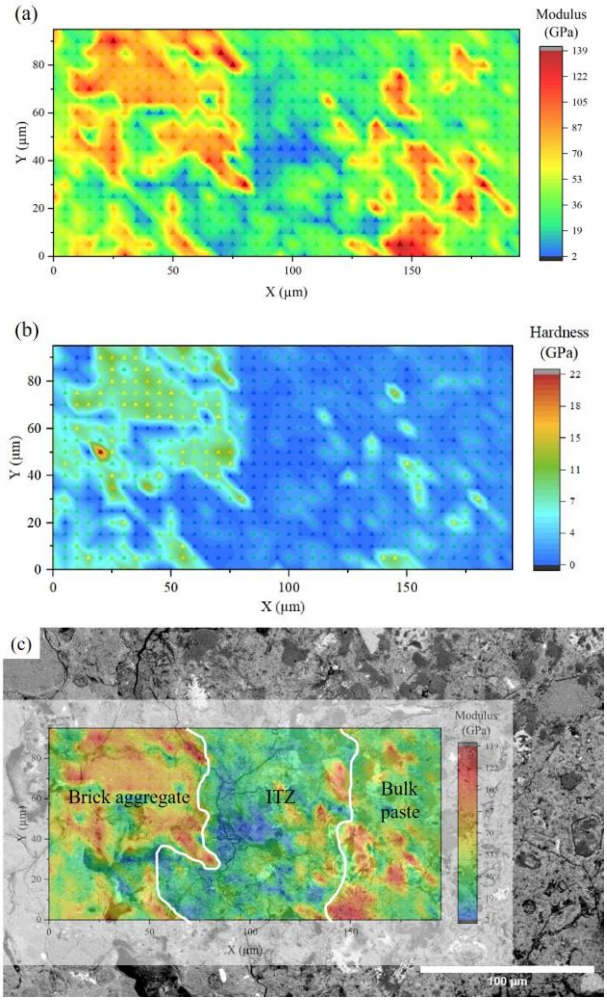

Figure 5: The mapping of the indentation modulus (a) and the hardness (b) of the area around brick aggregate, and the overlapped SEM-BSE image with modulus mapping (c).

It can be observed that the M and H are high in the region from 0 up to 75 µm along the X-axis. Compared to **Fig. 2**, this region can be identified as brick aggregate with an average M of 59.6 ± 29.5 GPa and H of 5.5 ± 3.3 GPa. There is considerable variability in these values due to the presence of numerous air voids and high mechanical property quartz in the brick aggregate. The modulus mapping overlaid on the SEM-BSE image further confirms these observations, as the mapped morphology closely matches the SEM image. This configuration can better define the boundaries between aggregate, ITZ, and bulk paste, as shown in **Fig. 5c**. It can be observed that the lower M phases predominate in the vicinity of the aggregate, while the higher M phases predominate in regions further away from the interface.

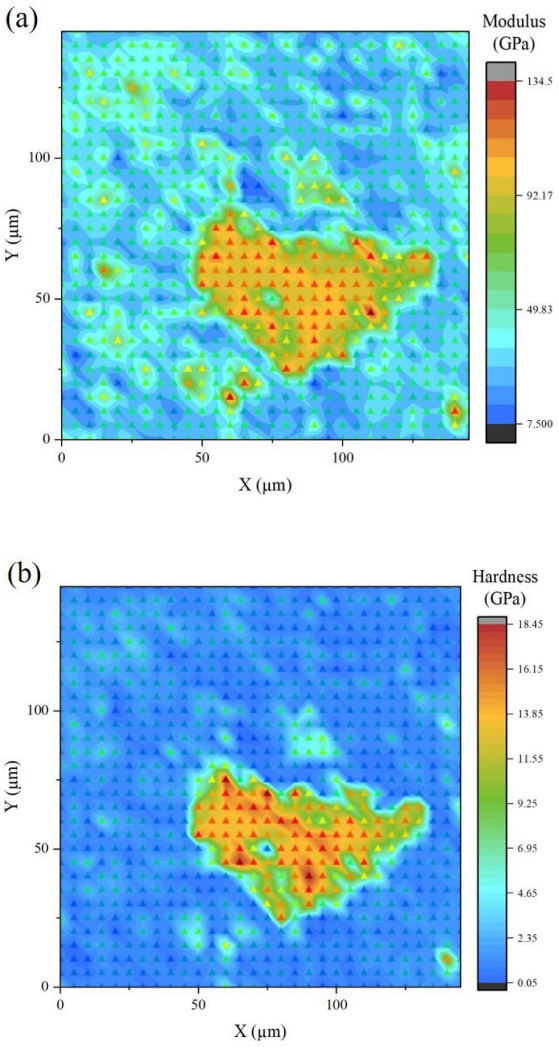

Figure 6: The mapping of indentation modulus (a) and hardness (b) in the bulk paste.

Fig. 6 shows the micromechanical properties in the bulk paste. A particle with high modulus (95.1 GPa) and hardness (12.7 GPa) occurs in the central region. According to **Fig. 4**, the particle can be identified as a sand powder with an approximate size of 80 µm. Notably, no apparent ITZ is found around this sand powder, suggesting that it is isolated from the cement paste microstructure.

3.3 Indentation analysis

Based on the measured indentation moduli, 780 indentations in ITZ and 716 indentations in bulk paste (excluding those associated with sand powder) were deconvoluted into 4 phases. The indentations in ITZ were taken from 3 different areas corresponding to a thickness of 65 µm. To facilitate a comparison with the ITZ, 716 indentations in the bulk paste were chosen using a region segmentation method, ensuring the exclusion of two distinct areas containing sand powder.The bin size was set to 2 GPa in the construction of the probability density functions (PDFs). The phases corresponding to the peaks are shown in **Fig. 7**.

According to the previous studies [12,15], they are identified as porosity, low density C-S-H (LD C-S-H), high density C-S-H (HD-C-S-H), and calcium hydroxide (CH). As presented in **Table 3**, the results of the deconvolution optimization process are summarized in terms of volume fraction and the average indentation modulus (M) for each phase. The indentation moduli of the 4 phases are in agreement with those reported in the literature [6,8,11,14-16].

Table 3: Results of deconvolution analysis in bulk paste and ITZ.

Phase	Bulk paste		ITZ	
	f^*(%)	M* (GPa)	f (%)	M (GPa)
Porosity	0	9.3	2.7	10.3
LD C-S-H	23.7	23.3	32.3	25.3
HD C-S-H	53.2	29.5	25.3	33.5
CH	23.1	40.5	39.7	43.7

* f: volume fraction; M: modulus of phase.

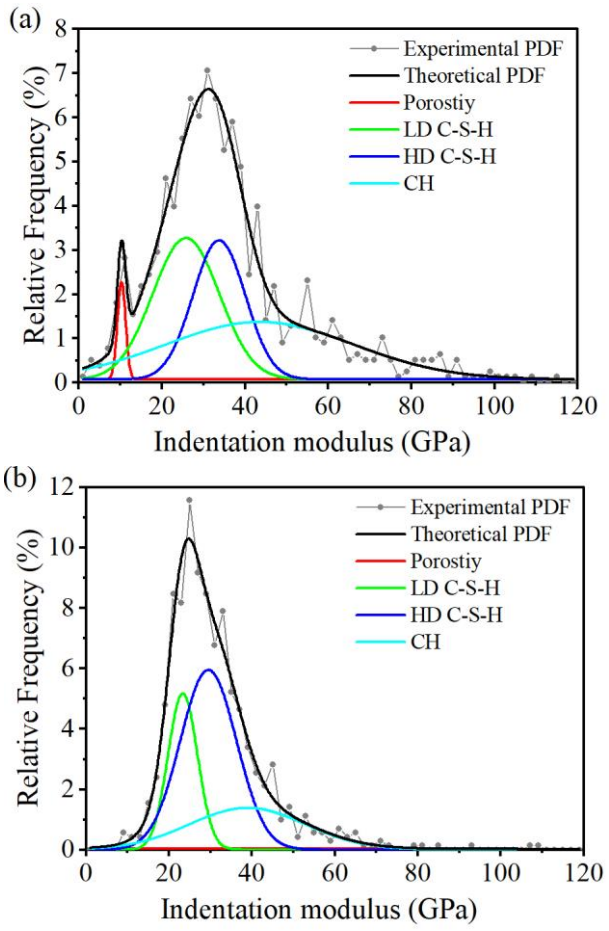

Figure 7: Deconvolution of frequency of indentation moduli from ITZ (a) and bulk paste (b).

In terms of volume fraction, there are significant differences between the ITZ and the bulk paste. Compared to the ITZ, the fractions of porosity, LD C-S-H, and CH in the bulk paste decreased, while the fractions of HD C-S-H increased. These results are consistent with the observations from the SEM images, where the ITZ has a higher porosity and a less compact microstructure than the bulk paste. This correlation further explains the lower micromechanical properties (modulus and hardness) in the ITZ compared to the bulk paste.

It is important to note that nanoindentation has inherent limitations in detecting certain microstructural phases, such as pore and residual cement clinker. The minimal presence of residual cement clinker (see Fig. 2 and 4) limits its identification during deconvolution. However, due to its small volume fraction, its effect on the other phases is not significant.

The pores have no mechanical properties. The resin is actually embedded in the pores of sample. The resin has a modulus of 4.8 GPa and a hardness of 0.2 GPa through the nanoindentation test on the sample. The modulus and hardness of the pores counted in the ITZ and bulk paste region are about 10 GPa and 0.3 GPa, respectively. This indicates that the porosity also incorporates certain indents with modulus greater than 4.8 GPa. However, the porosity in the bulk paste is zero due to the insignificant peak in **Fig. 7b**.

The pixel size in the SEM image is 168 nm, and the indentation depth is at least 500 nm when the modulus is less than 10 GPa. Accordingly, the smallest pore that can be detected by nanoindentation is 500 nm, while by image analysis it is 168 nm. As a result, the porosity by indentation analysis is significantly lower than the porosity by image analysis.

4 CONCLUSIONS

The differences between the interfacial transition zone and the bulk paste were investigated on recycled concrete made from recycled brick aggregate using nanoindentation combined with SEM. The main conclusions are:

- The thickness of the ITZ of the brick aggregate was measured to be 65 µm, as determined from the porosity distribution in the SEM-BSE images. The porosity of the ITZ of the brick aggregate was found to be twice that of the bulk paste.
- The morphological characteristics measured by grid nanoindentation are comparable to those in the SEM-BSE images. This allows for the combination of SEM and nanoindentation to determine the exact position of the indentations.
- A total of 780 indentations were examined within the three ITZs and a further 716 indentations were examined in the bulk paste. Deconvolution allows the classification of these indentations into four separate phases: porosity, low density calcium silicate hydrate (LD C-S-H), high density calcium silicate hydrate (HD C-S-H) and calcium hydroxide (CH). The volume fractions of the phases differ significantly between the ITZ and the bulk paste. The bulk paste has lower fractions of porosity, LD C-S-H and CH than the ITZ, but higher fractions of HD C-S-H.

REFERENCES

[1] S. Mindess and J. F. Young, *Concrete*. Prentice-Hall, 1981.

[2] S. Diamond, “The microstructure of cement paste and concrete—a visual primer,” *Cement and Concrete Composites*, vol. 26, no. 8, pp. 919–933, Nov. 2004, doi: 10.1016/j.cemconcomp.2004.02.028.

[3] A. Elsharief, M. D. Cohen, and J. Olek, “Influence of aggregate size, water cement ratio and age on the microstructure of the interfacial transition zone,” *Cement and Concrete Research*, vol. 33, no. 11, pp. 1837–1849, Nov. 2003, doi: 10.1016/S0008-8846(03)00205-9.

[4] Y. Gao, G. De Schutter, G. Ye, H. Huang, Z. Tan, and K. Wu, “Porosity characterization of ITZ in cementitious composites: Concentric expansion and overflow criterion,” *Construction and Building Materials*, vol. 38, pp. 1051–1057, Jan. 2013, doi: 10.1016/j.conbuildmat.2012.09.047.

[5] W. C. Oliver and G. M. Pharr, “An improved technique for determining hardness and elastic modulus using load and displacement sensing indentation experiments,” *Journal of Materials Research*, vol. 7, no. 6, pp. 1564–1583, Jun. 1992, doi: 10.1557/JMR.1992.1564.

[6] P. Acker, “Micromechanical analysis of creep and shrinkage mechanisms. In International conference on creep, shrinkage and durability mechanics of concrete and other quasi-brittle materials; Creep, shrinkage and durability mechanics of concrete and other quasi-brittle materials (pp. 15-26). Elsevier.,” presented at the International conference on creep, shrinkage and durability mechanics of

concrete and other quasi-brittle materials, Cambridge, MA: Elsevier, 2001, pp. 15–26.

[7] G. Constantinides and F.-J. Ulm, “The effect of two types of C-S-H on the elasticity of cement-based materials: Results from nanoindentation and micromechanical modeling,” *Cement and Concrete Research*, vol. 34, no. 1, pp. 67–80, Jan. 2004, doi: 10.1016/S0008-8846(03)00230-8.

[8] M. J. DeJong and F.-J. Ulm, “The nanogranular behavior of C-S-H at elevated temperatures (up to 700 °C),” *Cement and Concrete Research*, vol. 37, no. 1, pp. 1–12, Jan. 2007, doi: 10.1016/j.cemconres.2006.09.006.

[9] J. Xiao, W. Li, Z. Sun, D. A. Lange, and S. P. Shah, “Properties of interfacial transition zones in recycled aggregate concrete tested by nanoindentation,” *Cement and Concrete Composites*, vol. 37, pp. 276–292, Mar. 2013, doi: 10.1016/j.cemconcomp.2013.01.006.

[10] E. Donnelly, S. P. Baker, A. L. Boskey, and M. C. H. van der Meulen, “Effects of surface roughness and maximum load on the mechanical properties of cancellous bone measured by nanoindentation,” *Journal of Biomedical Materials Research Part A*, vol. 77A, no. 2, pp. 426–435, 2006, doi: 10.1002/jbm.a.30633.

[11] L. Sorelli, G. Constantinides, F.-J. Ulm, and F. Toutlemonde, “The nano-mechanical signature of Ultra High Performance Concrete by statistical nanoindentation techniques,” *Cement and Concrete Research*, vol. 38, no. 12, pp. 1447–1456, Dec. 2008, doi: 10.1016/j.cemconres.2008.09.002.

[12] M. Vandamme, F.-J. Ulm, and P. Fonollosa, “Nanogranular packing of C–S–H at substochiometric conditions,” *Cement and Concrete Research*, vol. 40, no. 1, pp. 14–26, Jan. 2010, doi: 10.1016/j.cemconres.2009.09.017.

[13] J. Němeček, J. Lukeš, and J. Němeček, “High-speed mechanical mapping of blended cement pastes and its comparison with standard modes of nanoindentation,” *Materials Today Communications*, vol. 23, p. 100806, Jun. 2020, doi: 10.1016/j.mtcomm.2019.100806.

[14] G. Constantinides and F.-J. Ulm, “The nanogranular nature of C–S–H,” *Journal of the Mechanics and Physics of Solids*, vol. 55, no. 1, pp. 64–90, Jan. 2007, doi: 10.1016/j.jmps.2006.06.003.

[15] K. Velez, S. Maximilien, D. Damidot, G. Fantozzi, and F. Sorrentino, “Determination by nanoindentation of elastic modulus and hardness of pure constituents of Portland cement clinker,” *Cement and Concrete Research*, vol. 31, no. 4, pp. 555–561, Apr. 2001, doi: 10.1016/S0008-8846(00)00505-6.

[16] X. Wang, S. Dong, Z. Li, B. Han, and J. Ou, “Nanomechanical Characteristics of Interfacial Transition Zone in Nano-Engineered Concrete,” *Engineering*, vol. 17, pp. 99–109, Oct. 2022, doi: 10.1016/j.eng.2020.08.025.